Computer Methods in Biomechanics and Biomedical Engineering
Vol. 11, No. 6, December 2008, 641–648

Taylor & Francis
Taylor & Francis Group

TECHNICAL NOTE

The static accuracy and calibration of inertial measurement units for 3D orientation

M.A. Brodie*, A. Walmsley and W. Page

Institute of Food, Nutrition and Human Health, Massey University, Wellington, New Zealand

(*Received 1 November 2006; final version received 23 October 2007*)

Inertial measurement units (IMUs) are integrated electronic devices that contain accelerometers, magnetometers and gyroscopes. Wearable motion capture systems based on IMUs have been advertised as alternatives to optical motion capture. In this paper, the accuracy of five different IMUs of the same type in measuring 3D orientation in static situations, as well as the calibration of the accelerometers and magnetometers within the IMUs, has been investigated. The maximum absolute static orientation error was 5.2°, higher than the 1° claimed by the vendor. If the IMUs are re-calibrated at the time of measurement with the re-calibration procedure described in this paper, it is possible to obtain an error of less than 1°, in agreement with the vendor's specifications (XSens Technologies B.V. 2005. Motion tracker technical documentation Mtx-B. Version 1.03. Available from: www.xsens.com). The new calibration appears to be valid for at least 22 days providing the sensor is not exposed to high impacts. However, if several sensors are 'daisy chained' together changes to the magnetometer bias can cause heading errors of up to 15°. The results demonstrate the non-linear relationship between the vendor's orthogonality claim of $< 0.1°$ and the accuracy of 3D orientation obtained from factory calibrated IMUs in static situations. The authors hypothesise that the high magnetic dip (64°) in our laboratory may have exacerbated the errors reported. For biomechanical research, small relative movements of a body segment from a calibrated position are likely to be more accurate than large scale global motion that may have an error of up to 9.8°.

Keywords: inertial measurement units; accelerometer; gyroscope; magnetometer; XSens; calibration

Introduction

Wearable motion capture systems based on inertial measurement units (IMUs) have become increasingly popular for the biomechanical analysis of human movement. However, there is very little information available about the intrinsic accuracy of such systems and the robustness of the methods used to calculate 3D orientation from the raw data in different situations.

This paper reports the accuracy of 3D orientation obtained from IMUs in static situations when rotated through a set of precisely known orientations. Because all other sources of error, such as soft tissue artefacts and Kalman filter lag, are removed, it is possible to investigate and then reduce the underlying causes of the orientation error. In a clinical situation static orientation accuracy may be important in applications such as determining the range of motion of subjects in rehabilitation programs. Assessment and improvement of the dynamic accuracy of IMUs will be presented in a companion paper.

At the 2007 International Society of Biomechanics Congress held in Taiwan, there were several papers that reported the use of IMUs for biomechanical analysis in diverse scenarios ranging from ski jumping (Ohgi et al. 2007) to rehabilitation (Cutti et al. 2007). The accuracy of the results reported in these papers was variable. In many cases, the authors employed ingenious methods, such as post filtering (Brodie et al. 2007) or attaching a small additional camera to the subject (Dutta et al. 2007), to get meaningful information from the sensors. In other cases, the authors reported highly accurate results (using a Kalman Filter solution) (Baten 2007, Koopman et al. 2007, Vries et al. 2007 and Petrone 2007). This suggests that the accuracy of the sensors may be dependant on the particular application. Papers that investigated slow steady movements that occurred in a short time frame or were constrained to single planes of motion were, in general, more successful than investigations into faster, continuous or unpredictable movements that occurred through a large volume.

The variability in accuracy of orientation data is reflected in the published literature. Giansanti et al. (2007) used IMUs to measure trunk orientation in the sit-to-stand task. The authors reported a maximum orientation error of 0.5° in trunk pitch and a maximum positional error of 5.6 mm. The high accuracy may have been achieved because the movement occurred in less than 4 s, the movement was constrained to trunk rotation about the mediolateral axis (pitch), and the IMU algorithm parameters were optimised on 30 healthy volunteers

*Corresponding author. Email: m.a.brodie@massey.ac.nz

ISSN 1025-5842 print/ISSN 1476-8259 online

DOI: 10.1080/10255840802326736
http://www.informaworld.com

prior to testing. In contrast, Pfau et al. (2005) used IMUs to measure the dynamic orientation and linear displacement of a horse's trunk during cantering. In this paper, the orientation error was reported as a median error, the worst case being 5.4° about the roll axis, with a range of motion of 12.5° (a median error of 43%). Consequently, it is likely the maximum error was considerably larger. Accurate displacement data were obtained by high pass filtering in combination with the assumption that the horse was running at constant speed on a treadmill.

The MT9 IMU

All the IMUs used in the experiments reported here were MT9 sensors (serial numbers MT7315–MT7319) from XSens Technologies, Enschede, The Netherlands. An IMU capable of 3D motion capture over an extended time frame requires three accelerometers, three magnetometers and three gyroscopes, one of each type of sensor for each of three orthogonal axes. The MT9 sensor actually contains three uniaxial gyroscopes (XRS300ABG), two biaxial accelerometers (AD218JE), one uniaxial magnetometer (KMZ51), one biaxial magnetometer (KMZ41) and one thermometer. The MT9 also contains all the necessary analogue and digital electronics to interface the sensors. The MT9 housing measures 53.5 mm long by 38.5 mm wide by 28.7 mm high and the unit weighs 35 g.

The conditioning applied to the raw signals is contained in proprietary firmware incorporated into the sensor and the output supplied contains 11 channels; a time stamp, three accelerometer channels, three gyroscope channels, three magnetometer channels and a thermometer. Details about the quality of the data from each of these channels are available from XSens who supply a factory calibration sheet with each IMU. Of interest is the reported bias stability, $5\,\mathrm{deg\,s^{-1}}$ for the gyroscopes, $0.02\,\mathrm{m\,s^{-2}}$ for the accelerometers and 0.5 m gauss for the magnetometers. Also of interest is the performance specification of the unit as a whole; static accuracy of orientation is reported to be $<1.0°$, dynamic accuracy 3° RMS and orthogonality of 0.1° (XSens Technologies B.V. 2005). These specifications come with the caveat, in the fine print, that data must be captured in a homogeneous magnetic environment and may depend on the type of motion measured. However, no details are given about what is an acceptable 'type of motion' and hence, given our experience, we consider that the manufacturer, at the time the manual was written, was unsure of what 'type of motion' could be measured accurately.

Up to 10 MT9 sensors can be connected to an XBus Master that synchronises measurements and compiles a single binary message for all connected sensors at each epoch. The XBus Master has two input channels and sensors, if more than two sensors are required they may be connected in a 'daisy chain' to each channel.

Obtaining a static estimate of orientation

Determination of sensor orientation requires the rotation in each of three rotational degrees of freedom to be specified. In static situations, the accelerometers and magnetometers each allow the definition of two orthogonal rotational axes. Therefore, orientation may be defined in two different ways, either a magnetometer-based (provided the angle of magnetic dip is known) or an accelerometer-based estimate.

The accelerometers define the orientation of the resultant acceleration vector, and if the sensor is static this corresponds to the orientation of the Earth's gravitational field (the global Z-axis) as measured in the local sensor coordinate system. With two degrees of freedom defined, the local coordinate system could still rotate in the horizontal plane about the global Z-axis to an infinite number of orientations as we have only defined the pitch and roll of the sensor. To obtain a heading fix the magnetometers are used. The magnetometers define the Earth's magnetic field vector as measured in the local sensor coordinate system. Using only the magnetometer channels, we may define the heading and pitch axes of the sensor (relative to the magnetic dip) but not the roll. Combining accelerometer and magnetometer data allow the definition of a global coordinate system (Figure 1), and Equations (1)–(6) demonstrate how to calculate an accelerometer-based static orientation matrix ($\mathbf{R}_{LG}$).

The direction of Earth's gravitational field in local coordinates, the coordinates of the IMU, is represented by the vector ($\mathbf{Z}_{Local}$), Equation (1). The local acceleration vector is calculated by normalising the accelerometer channels (Ax, Ay and Az), Equation (2)

$$\mathbf{Z}_{Local} = \begin{bmatrix} Zx \\ Zy \\ Zz \end{bmatrix}, \tag{1}$$

$$Zx = \frac{Ax}{\sqrt{Ax^2 + Ay^2 + Az^2}} = \frac{Ax}{|\mathrm{A}|}. \tag{2}$$

In a similar way, the direction of the Earth's magnetic field in local coordinates ($\mathbf{H}_{Local}$) is calculated from the

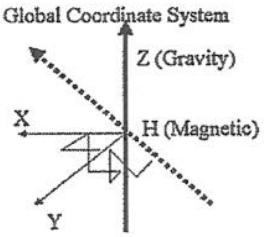

Figure 1. Diagram of the global coordinate system.

magnetometer channels (*hx*, *hy* and *hz*), Equation (3)

$$\mathbf{H}_{\text{Local}} = \frac{\mathbf{h}}{|\mathbf{h}|}. \quad (3)$$

The local *Y*-axis ($\mathbf{Y}_{\text{Local}}$) is defined as the vector that is mutually perpendicular to both the local magnetic field vector and the local gravitational field vector. It is therefore found by the cross product of these two vectors, Equation (4)

$$\mathbf{Y}_{\text{Local}} = \mathbf{Z}_{\text{Local}} \times \mathbf{H}_{\text{Local}}. \quad (4)$$

The local *X*-axis (X_{Local}) is defined as the vector that is normal to both the local *Y*-axis and the local gravitational field, Equation (5)

$$\mathbf{X}_{\text{Local}} = \mathbf{Y}_{\text{Local}} \times \mathbf{Z}_{\text{Local}}. \quad (5)$$

The orientation matrix ($\mathbf{R}_{\text{Local to Global}}$) describes the sensor orientation in the global reference frame and can be computed from the local axes, Equation (6)

$$\mathbf{R}_{LG} = \begin{bmatrix} \mathbf{X}_{\text{Local}} & \mathbf{Y}_{\text{Local}} & \mathbf{Z}_{\text{Local}} \end{bmatrix}. \quad (6)$$

The global coordinate system used by the IMUs is the *Z*-axis points vertically upwards, the *X*-axis points to magnetic north and is normal to the *Z*-axis and the *Y*-axis is normal to both *X*- and *Z*-axes. In static situations, the specification indicates that the orientation of the sensor given by the manufacturer's rotation matrix ($\mathbf{R}_{LG}$) is accurate to within 1°. However, if there is significant noise in one or all of the magnetometer or accelerometer channels, it is unlikely that the mean of the calculated $\mathbf{R}_{LG}$ will approximate the true rotation matrix because of the non-linear calculation procedure required to obtain $\mathbf{R}_{LG}$. The calculation produces unpredictable results near the Earth's magnetic poles, in situations of free fall, when the sensor is accelerating, or moving at constant velocity in a non-uniform magnetic field.

Any measurement in the local coordinate system may be converted to the global coordinate system by multiplication of the measurement by the rotation matrix, Equation (7)

$$\mathbf{H}_{\text{Global}} = \mathbf{R}_{LG}\mathbf{H}_{\text{Local}}. \quad (7)$$

Method

Experiments were designed to determine the absolute and relative accuracy of IMU-based static orientation measurements; the precision of such measurements; the improvement in accuracy that could be made by using a custom calibration procedure and the stability of measurements over several days using the custom calibration procedure.

The static calibration rig

A static calibration rig was constructed from non-magnetic material. The calibration rig consisted of a precisely machined box with vertices of 90°, the internal faces parallel to the external faces and a flat, level platform. The IMU was clamped inside the box by two non-metallic securing screws. The box was then turned through 24 right-angle rotations on the rig platform which was aligned with the global coordinate system, Figure 2.

The vertices of the box housing the IMU were tested with an engineer's square and within the visible limits of the square were 90°. The box was manufactured with a corner slot to prevent the connecting cable from interfering with the rotations. Two securing screws on perpendicular faces of the box ensured that the IMU was held against the same two internal faces of the box without the possibility of movement.

The rig platform had a fixed bar that the box containing the IMU was rested against to ensure repeatability of box orientation. The rig platform was aligned with the global coordinate system with a compass and spirit level. The base of the compass rested against the platform bar and the platform was rotated until it was aligned with magnetic north. The reading error of the compass was ±1°. The rig platform was levelled using a spirit level. To ensure the platform was level, the procedure was repeated several times, each time turning the spirit level by 180°. This procedure was repeated for both the *x*- and *y*-axes of the platform. It was found that 1/8th of a turn to an adjustment screw produced a just perceptible change to the spirit level. This corresponded to a change in height of 0.3 mm over 100 mm, the minimum distance between the screws, or an angular change of approximately 0.2°.

Trials

Each trial consisted of the complete set of 24 orthogonal orientations of the sensor in the calibration rig. Each measurement was separated by at least 90° from any other measurement. Before each measurement, the IMU was

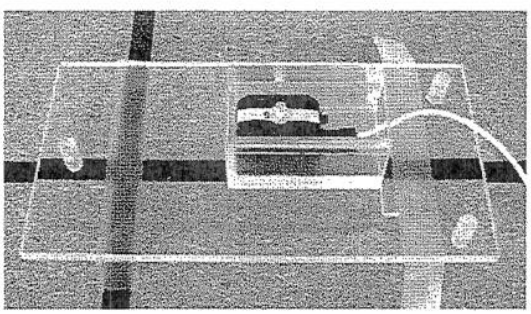

Figure 2. The static calibration rig.

allowed to settle for 1 s and then 1 s of raw binary data were collected at 100 Hz using a MATLAB programme. The raw binary data were converted to calibrated data using both the factory supplied calibration and our own custom calibration. The measured calibrated data consisted of three accelerometer channels and three magnetometer channels. The first and last 10 data points from each measurement were discarded and the mean of the remaining data for each channel was used to calculate the static orientation of the IMU at each measured orientation.

During the trials, all magnetic objects except for the sensors themselves were removed from the test area. The sensor temperature was allowed to stabilise between 28.5 and 29.5°C before each test to remove the possibility of temperature related drift. Although in principle this is unnecessary because temperature compensation is applied when converting the raw binary data to calibrated data.

Quaternion representation and error calculation

Quaternion representation is used to report the orientation error in terms of the magnitude of a single rotation (θ_{12}) that separates the measured 3D orientation from the 'true' orientation, Equation (10). Quaternion representation of orientation has four components, one real and three imaginary, in vector form. The imaginary parts contain the x, y and z components of a unit vector ($\mathbf{U}$) while the real part of the quaternion defines a rotation (θ) about $\mathbf{U}$, Equation (8)

$$\mathbf{Q} = \left[\cos(\theta/2) \quad \mathbf{U}x\sin(\theta/2) \quad \mathbf{U}y\sin(\theta/2) \quad \mathbf{U}z\sin(\theta/2)\right], \tag{8}$$

$$\mathbf{Q}_{12} = \mathbf{Q}_2 * \mathbf{Q}_1^{-1}, \tag{9}$$

$$\theta_{12} = 2*\cos^{-1}\mathbf{Q}_{12}[1], \tag{10}$$

$$\theta_{\text{Comp}} = \frac{\theta_{12}}{\sin(\theta_{12}/2)} * \mathbf{Q}_{12}[2 \quad 3 \quad 4]. \tag{11}$$

The difference between two orientations in the global coordinate system, $\mathbf{Q}_{12}$, can be calculated by quaternion multiplication (which is different to normal matrix multiplication) of $\mathbf{Q}_2$ by the inverse of $\mathbf{Q}_1$, Equation (9). By definition the inverse quaternion is the original quaternion with the sign of the real element inverted. From the real element of $\mathbf{Q}_{12}$, the smallest angle between the two quaternions can be calculated, Equation (10). Care must be taken to choose the smaller absolute value of the two possible outcomes because a rotation greater than 180° can also be represented as a negative rotation which is equivalent to a positive rotation about $-\mathbf{U}$. Finally, the components of the angular error, θ_{Comp}, about the global axes can then be calculated by Equation (11).

Statistics

A trial consisted of 24 separate measurements from a single sensor at different orientations as described above. For each trial, the root mean square (RMS) error was calculated. The RMS error was used because representation of orientation by quaternions resulted in both positive and negative angular error. The arithmetic mean could result in an error value close to zero, which would overestimate the average variability of the sensor over the 24 separate measurements.

Where multiple trials with one or more sensors were grouped for analysis, the RMS values from each individual trial were averaged and reported as the Mean RMS error, representing the average performance over multiple trials for the experimental condition. The maximum value reported is the worst-case error of a single measurement, while the minimum is the best-case error in orientation from a single measurement.

Calibration of the IMU raw data

The raw data from the IMU are output as a binary message (called MID50 by the manufacturer), and the format of the message is available from XSens Technologies B.V. (2004a). The sensors in the MT9 unit have bandwidths of 0–50 Hz for the gyroscopes, 0–30 Hz for the accelerometers and 0–10 Hz for the magnetometers. The raw binary data are transformed into calibrated floating point data by converting the measured binary data to an integer then applying the appropriate bias, gain, misalignment and temperature compensation to get a floating point representation of the various IMU channels. This is done automatically in the MT9 firmware; Equation (12) describes the integer to floating point data calibration. Alternatively, it is possible to access the calibration parameters directly from each sensor using the XSens binary communication protocol and then uses the raw binary data directly for biomechanical analysis. The format of the calibration messages (MID145) and instructions for processing the raw binary data is available from XSens Technologies B.V. (2004b). A calibration algorithm was supplied with the MT9 software but it only re-calibrated the accelerometer and gyroscope bias and did not significantly improve the accuracy of the IMUs. Therefore, the following custom calibration procedure was utilised.

Re-calibration of the accelerometer and magnetometer gain Go, bias bo and misalignment $\mathbf{R}$ can be achieved by comparing several expected measurements $\mathbf{S}$ in the calibration rig with the measured integer signal from each channel $\mathbf{U}$. For example, if the z-axis of the IMU is up

in the calibration rig the expected accelerometer vector $\mathbf{S} = [0\,0\,9.81]\,\mathrm{m\,s^{-2}}$ should be obtained from **U** following application of Equation (12)

$$\mathbf{S} = [\mathrm{Go}(\mathbf{I} + \mathrm{GT}(T - T_o))\mathbf{R}]^{-1}[\mathbf{U} - \mathrm{bo} - \mathrm{bT}(T - T_o)], \tag{12}$$

where bT, temperature offset; GT, temperature gain; T_o, reference temperature (35°C); T, sensor temperature and **I**, 3 × 3 identity matrix. Equation (12) can be reformulated to the to solve for a variable X which contains the gains, bias and misalignment in a single 3 × 4 matrix (Equation (13)). An additional row vector of ones, **ONES**, of the length **U** is added to right side of the equation so that the bias will be included in the solution of X. The authors found using the full set of 24 orthogonal rotations provided the best calibration. As there are 12 unknowns the system of equations is over determined and hence a least-squares solution may be obtained using the generalised (Moore–Penrose) inverse and Equation (13)

$$X = [[\mathbf{I} + \mathrm{GT}(T - T_o)]{*}\mathbf{S}] \Big/ \begin{bmatrix} \mathbf{U} - \mathrm{bT}(T - T_o) \\ \mathbf{ONES} \end{bmatrix}, \tag{13}$$

$$X = \begin{bmatrix} [\mathrm{GoR}]^{-1} & \mathbf{E} \end{bmatrix}, \tag{14}$$

$$\mathrm{bo} = -\mathrm{GoR}{*}\mathbf{E}. \tag{15}$$

The gains (Go), misalignment (**R**) and bias (bo) are extracted from the solution (X) by Equations (14) and (15). In this case, GoR is a 3 × 3 matrix and **E** is a three element column vector. Because the gain and misalignment matrices are mutually dependant, one solution for the gains is to make Go the diagonal of GoR and **R** then becomes the residual.

Experiments

Four experiments were performed to investigate IMU measurement accuracy, precision and stability.

Experiment 1

The absolute accuracy of IMUs in determining orientation relative to the global reference frame (Table 1).

The data from five different IMUs (serial numbers MT7315–MT7319) were collected at each of the 24 orthogonal orientations in the global reference system. Measurements of IMU orientation (120 in total) were compared against the known orientation of the IMU in the calibration frame to investigate the magnitude and spread of the error in absolute orientation. Absolute orientation is less important in biomechanics but more important for navigational systems. In column 1, the orientation error of all sensors is calculated based on the factory calibration of the raw binary data. In columns 3–6, the orientation error of all sensors from days 1 to 22 is calculated using the custom calibration completed on day 1 to process the raw binary data. In the last three rows, the total error was split into component rotations about the global axis to further understand the sources of the orientation error. Column 2 contains the orientation errors of all the sensors excluding sensor MT7315 based on the factory calibration.

Experiment 2

The relative accuracy of the IMU in determining orientation relative to the IMU start position (Table 2).

The same five sensors from experiment 1 were used but this time the sensor orientation in the start position was mapped to the known orientation of the calibration rig, so there would be zero error in the start position. The relative measured IMU orientation at each of the 24 orthogonal orientations was then compared to known relative orientation and the error calculated. This procedure is similar to the protocol required in the biomechanical analysis of human motion in which each sensor must be mapped to the 'rigid' body segment to which it is attached in an initial calibration procedure.

Experiment 3

The intra-sensor precision (Table 3).

Table 1. The absolute accuracy of the IMU sensors, Experiment 1.

	Factory calibration		Re-calibrated all sensors			
$n = 120$ (5 × 24)	All sensors	No MT7315	Day 1	Day 2	Day 3	Day 22
Mean (RMS °)	6.1	3.0	0.36	0.57	0.78	0.55
Standard deviation (°)	4.5	1.2	0.18	0.36	0.52	0.31
Maximum (°)	21.6	5.2	0.84	1.7	2.0	1.7
Minimum (°)	0.80	0.8	0.07	0.05	0.03	0.02
Component angles (mean RMS)						
X-axis (roll °)	2.2	0.92	0.06	0.14	0.13	0.16
Y-axis (pitch °)	2.2	0.92	0.09	0.15	0.13	0.15
Z-axis (yaw °)	5.2	2.68	0.34	0.53	0.76	0.51

Table 2. The relative accuracy of the IMU sensors, Experiment 2.

	Factory calibration		Re-calibrated all sensors			
$n = 120$ (5 × 24)	All sensors	No MT7315	Day 1	Day 2	Day 3	Day 22
Mean (RMS °)	6.9	4.5	0.42	0.72	0.86	0.76
Standard deviation (°)	4.6	2.5	0.23	0.46	0.54	0.47
Maximum (°)	24.5	9.8	1.1	2.4	2.2	2.5
Minimum (°)	0	0	0	0	0	0

The intra-sensor precision for static orientation measurements was examined by three repeat trials of 24 orthogonal rotations with the five different sensors (360 measurements in total). The error for each measurement was calculated as the difference of the measured orientation by each sensor from the mean as measured by each sensor at each orthogonal rotation.

Experiment 4

The 'daisy chain' effect (Table 4).

The authors hypothesised that connecting several sensors together on a daisy chain to a single channel of the XBus Master might effect the current flowing through the connections of each sensor and hence the magnetometer calibration. In this experiment, a single sensor was fastened to a flat surface with up to four additional sensors attached to it in a daisy chain. Next, the nominal power draw from additional sensors on the daisy chain was simulated (40 mA/sensor) by adding additional resistance across the male connector of the MT9 sensor. Changes in local magnetometer output, heading of the sensor, current into the sensor and voltage across the sensor were recorded.

Results

See Tables 1–4.

Discussion

The absolute error of the five IMUs tested relative to the global coordinate system was investigated and the results presented in Table 1. Excluding sensor MT7315, the RMS error in absolute orientation with factory calibration was 3° and the maximum error was 5.2°. This is larger than the value published by the manufacturer of less than 1° in static situations. After recalibration of the accelerometers and magnetometers by the method presented in this paper, the mean RMS error dropped to 0.36° and the maximum error dropped to 0.86°. The result, including sensor MT7315, suggests that frequent recalibration of the accelerometers and magnetometers by the method presented in this paper may be required to achieve accurate results with IMUs.

The requirement for periodic recalibration over time was investigated by retesting the five IMUs 2, 3 and 22 days after the first experiment (see Table 1). For each test on each day, the binary data were processed using the custom calibration from day 1. The maximum error increased from 0.86° on day 1 (immediately following recalibration) to 2.0° on day 2, before dropping to 1.7° on day 22. The RMS error went from 0.36° on day 1 to 0.55° on day 22. The results suggest that the custom calibration is valid for at least 22 days provided the sensor is not subjected to substantial impacts. The slight increase in error from days 1 to 2 is possibly a consequence of the error, ± 1°, associated with alignment of the *x*-axis of the calibration rig with magnetic north each day.

The orientation error was further broken down into component rotations about the global *X*-, *Y*- and *Z*-axes to investigate the error source, Table 1. In all cases, the major component of error is rotation about the global *Z*-axis (heading error) approximately three times the error about either the *X*- or *Y*-axes. It would be reasonable to assume therefore that the magnetometers, responsible for heading, are less accurate than the accelerometers. However, heading is not calculated directly from the magnetometers, it is calculated from the cross product of the gravity vector and the local *y*-axis, a vector mutually perpendicular to both the gravity vector and the magnetic field vector. The accuracy of the heading therefore depends on the output from the accelerometers and magnetometers and there being sufficient angular separation between the magnetic field and the gravity vector to properly define the *y*-axis. The results show that even if the sensor orthogonality is the 0.1° claimed, the error (up to 5.2°), depends on the non-linear interaction between the magnetometer and accelerometer bias. In our laboratory, the magnetic dip angle is approximately 64° (latitude 41° south) resulting in a 36° separation between the magnetic field vector and the gravity vector and hence a roll error of 1°

Table 3. The intra-sensor precision, Experiment 3.

$n = 360$ (3 × 5 × 24)	Factory calibration five sensors repeated three times
Mean (RMS °)	0.13
Standard deviation (°)	0.08
Maximum (°)	0.56
Minimum (°)	0.01

Table 4. The daisy chain effect, Experiment 4.

	Extra sensors					Extra current through first sensor [mA]								
	0	1	2	3	4	0	40	80	120	160	200	240	280	320	360
Heading (°)	65.4	63.4	61.9	60.4	58.9	65.1	63.6	62.1	60.5	58.8	57.1	55.4	53.7	51.9	50.1
Heading error (°)	0.0	1.9	3.4	5.0	6.5	0.0	1.6	3.0	4.7	6.3	8.0	9.7	11.4	13.3	15.0
Magnotometer [T]															
Local *x*-axis	−0.38	−0.36	−0.35	−0.34	−0.33	−0.37	−0.36	−0.35	−0.34	−0.33	−0.32	−0.31	−0.30	−0.28	−0.27
Local *y*-axis	0.95	0.96	0.96	0.96	0.96	0.95	0.95	0.95	0.95	0.96	0.96	0.96	0.96	0.97	0.97
Local *z*-axis	0.19	0.20	0.20	0.21	0.22	0.19	0.20	0.20	0.21	0.22	0.23	0.23	0.24	0.25	0.26

produces an additional error in the heading of approximately 2°. The high angle of dip means that the horizontal component of the Earth's field is about 1/3 the total magnitude and therefore any magnetometer error will have a relatively greater effect on the heading measured in the horizontal plane. The magnetometers are sensitive to small fluctuations in the local magnetic field and these effects would be less significant if the angle of magnetic dip was closer to zero, as it is in lower latitudes.

To construct biomechanical models of human movement, the IMUs are attached to body segments in a systematic way so that the local coordinate system of the IMU with respect to the local coordinate system of the body segment is known. Usually a static calibration position is used to map the IMU to its attached body segment. Thus, the relative orientation from a known starting orientation may be more important than the absolute orientation in space. Using the factory calibration, the RMS and maximum error for relative orientation was 4.5° and 9.8°, respectively, Table 2. This is greater than the absolute error because the error in the initial orientation compounds the error in each of the subsequent 23 rotations of 90°. Recalibration improved the RMS and maximum error to 0.42° and 1.1°, respectively. On day 22, the RMS error had only increased slightly to 0.76° suggesting that for the majority of the measurements, especially if the motion only involves small deviations from the initial static calibration position, it should be possible to obtain a static accuracy within the manufacturers specifications of less than 1°.

The accuracy of the calibration rig orientation in the global coordinate system was estimated to be ±1° about each axis. The accuracy of the absolute orientation of the rig was confirmed by the low error in absolute orientation of the re-calibrated sensors on day 1, 0.36° RMS, Table 1. The repeatability of the rig to hold the sensor in the same position was confirmed by the low RMS error of 0.13° and a maximum error of 0.56° in the repeat trials, Table 3. This result also demonstrates that over a short period of less than 2 h, the IMU will produce highly repeatable static orientation results, even if it is poorly calibrated. As our experiments were conducted at constant temperature, the effectiveness of the internal temperature compensation could not be assessed.

Connecting several sensors to a single XBus Master in a daisy chain causes a bias error in the magnetometers, which results in up to 15° error in heading if nine extra IMUs are added, Table 4. It is likely that the extra current passing through the connectors of the first IMU due to the power draw of additional sensors in the daisy chain creates a local magnetic field. This affects the bias of the magnetometers because they are located close to the connectors. The hypothesis was confirmed by replacing the extra sensors in the daisy chain with resistors. The resistors simulated a nominal current of 40 mA per IMU. The magnetometer bias

could in theory produce a relative error of up to 30° if the sensor was rotated through 180° and both the start and the end orientations resulted in the bias vector being perpendicular to the global magnetic field. To mitigate the 'daisy chain' effect, the authors suggest calibrating the sensors daisy chained together as they would be in use. However, more research is required to determine if the effect is dependant on temperature or battery power.

Acknowledgements

We would like to thank Mike Turner for designing and building the calibration rig.

References

Baten CTM. 2007. Advancements in sensor based ambulatory 3D motion analysis. J Biomech. 40 (Supplement 2), S422.

Brodie M, Walmsley A, Page W. 2007. Fusion motion capture: The biomechanical analysis of alpine ski racing. J Biomech. 40(Supplement 2):S399.

Cutti AG, Giovanardi A, Rocchi L, Davalli A. 2007. Motion analysis of the upper limb based on inertial sensors: Part 1 – protocol description. J Biomech. 40(Supplement 2):S250.

Dutta T, Pham D, Fernie G. 2007. Predicting loads on the low back in the workplace: A wearable biomechanics lab. J Biomech. 40(Supplement 2):S114.

Giansanti D, Maccioni G, Benvenuti F, Macellari V. 2007. Inertial measurement units furnish accurate trunk trajectory reconstruction of the sit-to-stand manoeuvre in healthy subjects. Med Biol Eng Comput. 45(10):969–976.

Koopman H, Schepers H, Veltink P. 2007. Abulatory measurements require deformable foot models. J Biomech. 40(Supplement 2):S423.

Ohgi Y, Seo K, Hirai N, Murakami M. 2007. Aerodynamic forces acting in ski jumping. J Biomech. 40(Supplement 2):S399.

Petrone N. 2007. Aquisition and analysis of ground reaction forces and foot orientation on in line skates during track speed skating. J Biomech. 40(Supplement 2):S398.

Pfau T, Witte T, Wilson AM. 2005. A method for deriving displacement data during cyclical movement using as inertial sensor. J Exp Biol. 208:2503–2514.

Vries Wd, Veeger H, Baten C, Helm Fvd. 2007. Upper extremity load spectrum in daily situations: System accuracy and soft tissue artefacts. J Biomech. 40(Supplement 2):S424.

XSens Technologies B.V. 2004a. Technical documentation Xbus Master B. Version 1.32. Available from: www.xsens.com

XSens Technologies B.V. 2004b. Using motion tracker electronic data sheet (MTS Data). Version 1.1. Available from: www.xsens.com

XSens Technologies B.V. 2005. Motion tracker technical documentation Mtx-B. Version 1.03. Available from: www.xsens.com